

Influence of Spatial Variability on Slope Reliability Using 2-D Random Fields

D. V. Griffiths, F.ASCE¹; Jinsong Huang, M.ASCE²; and Gordon A. Fenton, M.ASCE³

Abstract: The paper investigates the probability of failure of slopes using both traditional and more advanced probabilistic analysis tools. The advanced method, called the random finite-element method, uses elastoplasticity in a finite-element model combined with random field theory in a Monte-Carlo framework. The traditional method, called the first-order reliability method, computes a reliability index which is the shortest distance (in units of directional equivalent standard deviations) from the equivalent mean-value point to the limit state surface and estimates the probability of failure from the reliability index. Numerical results show that simplified probabilistic analyses in which spatial variability of soil properties is not properly accounted for, can lead to unconservative estimates of the probability of failure if the coefficient of variation of the shear strength parameters exceeds a critical value. The influences of slope inclination, factor of safety (based on mean strength values), and cross correlation between strength parameters on this critical value have been investigated by parametric studies in this paper. The results indicate when probabilistic approaches, which do not model spatial variation, may lead to unconservative estimates of slope failure probability and when more advanced probabilistic methods are warranted.

DOI: 10.1061/(ASCE)GT.1943-5606.0000099

CE Database subject headings: Slope stability; Finite element method; Probability; Failures.

Introduction

Slope stability analysis is a branch of geotechnical engineering that is highly amenable to probabilistic treatment, and has received considerable attention in the literature. The earliest papers appeared in the 1970s [e.g., Matsuo and Kuroda (1974); Alonso (1976); Tang et al. (1976); and Vanmarcke (1977)] and have continued steadily [e.g., D'Andrea and Sangrey (1982); Chowdhury and Tang (1987); Li and Lumb (1987); Oka and Wu (1990); Mostyn and Li (1993); Lacasse (1994); Christian et al. (1994); Chowdhury and Xu (1995); Wolff (1996); Christian (1996); Lacasse and Nadim (1996); Low (1996); Low and Tang (1997a,b); Low et al. (1998); Hassan and Wolff (1999); Whitman (2000); Duncan (2000); El-Ramly et al. (2002); Low (2003); Bhattacharya et al. (2003); Griffiths and Fenton (2004); Babu and Mukesh (2004); Xu and Low (2006); Low et al. (2007); Cho (2007); and Shinoda (2007)]. In spite of this activity, the geotechnical profession is slow to adopt the probabilistic approaches to geotechnical design, especially in traditional problems such as slopes and foundations. In particular, while the importance of spatial correlation (or autocorrelation) and local averaging of statistical geotechnical properties have long been recognized by some investigators [e.g., Mostyn and Soo (1992)], it is still regu-

larly omitted from many probabilistic slope stability analyses. Griffiths and Fenton (2004) studied slope stabilities using random finite-element method (RFEM), which combines elastoplastic finite-element analysis with random fields generated using the local average subdivision method (Fenton and Vanmarcke 1990). The results indicated that traditional probabilistic analyses, in which spatial variability is ignored by implicitly assuming perfect correlation, can lead to unconservative estimates of the probability of failure. This paper thoroughly investigates this observation by assessing the influence of the spatial correlation length and coefficient of variation of strength parameters on slope stability across a wide range of parametric variations. Numerical results show that for a given value of the spatial correlation length, there is a critical value of the coefficient of variation of strength parameters, above which FORM, if spatial variation is not modeled, underestimates the probability of failure and is therefore unconservative. The influences of slope inclination, factor of safety (FS) (based on mean strength values), and cross correlation between strength parameters on the critical value of the coefficient of variation, have been investigated by parametric studies, indicating when more advanced probabilistic methods are warranted.

In spite of the fact that most traditional limit equilibrium methods (LEMs) existing in literature do not consider spatial variability, some investigators have combined the LEM with random field theory [e.g., Li and Lumb (1987); Mostyn and Soo (1992); Low and Tang (1997a,b); El-Ramly et al. (2002); Low (2003); Babu and Mukesh (2004); Low et al. (2007); Cho (2007); and Theory manual of slope/W 2007 version (2007)]. However, the inherent nature of LEM is that it leads to a critical failure surface, which in 2-D analysis appears as a line which could be noncircular. The influence of the random field is only taken into account along the line and is therefore one-dimensional. All results obtained by the previously mentioned implementations indicate that increasing the spatial correlation length leads to an increased probability of failure irrespective of the variance of the shear strength parameters. Some of the results presented in the current paper however,

¹Professor, Div. of Engineering, Colorado School of Mines, Golden, CO 80401. E-mail: d.v.griffiths@mines.edu

²Associate Research Professor, Div. of Engineering, Colorado School of Mines, Golden, CO 80401 (corresponding author). E-mail: jhuang@mines.edu

³Professor, Dept. of Engineering Mathematics, Dalhousie Univ., P.O. Box 1000, Halifax, N.S., Canada B3J 2X4. E-mail: gordon.fenton@dal.ca

Note. This manuscript was submitted on July 18, 2008; approved on February 9, 2009; published online on February 23, 2009. Discussion period open until March 1, 2010; separate discussions must be submitted for individual papers. This paper is part of the *Journal of Geotechnical and Geoenvironmental Engineering*, Vol. 135, No. 10, October 1, 2009. ©ASCE, ISSN 1090-0241/2009/10-1367-1378/\$25.00.

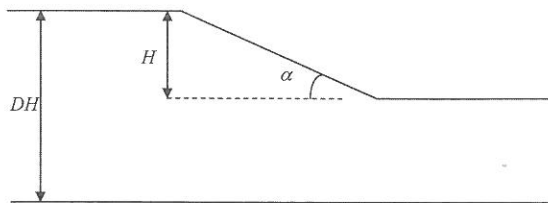


Fig. 1. Slope profile

indicate that both the spatial correlation length and the input vari-
ances can affect the probability of failure.

Both undrained $\phi_u=0$ and drained $c', \tan \phi'$ slopes are con-
sidered with the slope profile shown in Fig. 1. In this study, the
slope has height $H=10.0$ m, foundation depth ratio $D=2$, and soil
unit weight, γ_{sat} (or γ) $=20.0$ kN/m³, which are all held constant.
For undrained slopes, the shear strength c_u is assumed to be a
random variable and expressed in a dimensionless form given by
 $C_u = c_u / (\gamma_{\text{sat}} H)$. For drained slopes, both the shear strength c' ,
expressed in the dimensionless form $C' = c' / (\gamma H)$ and the tangent
of the friction angle, $\tan \phi'$, are assumed to be random variables.
Three different slope angles α are considered: $\alpha=18.4^\circ$ (3:1
slope), $\alpha=26.6^\circ$ (2:1 slope), and $\alpha=45^\circ$ (1:1 slope).

Probabilistic Descriptions of Strength Parameters

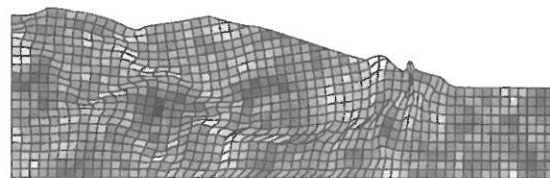
In this study, the shear strength parameters C_u , C' , and $\tan \phi'$ are
assumed to be random variables characterized statistically by log-
normal distributions (i.e., the logarithms of the properties are nor-
mally distributed). The lognormal distribution will be applied at
the point level. The lognormal distribution is one of many pos-
sible choices [e.g., Fenton and Griffiths (2008)], however, it of-
fers the advantage of simplicity, in that it is arrived by a simple
nonlinear transformation of the classical normal (Gaussian) dis-
tribution. Lognormal distributions guarantee that the random vari-
able is always positive and, in addition to the current writers, it
has been advocated and used by several other investigators as a
reasonable model for physical soil properties [e.g., Parkin et al.
(1988); Parkin and Robinson (1992); Nour et al. (2002); and
Massih et al. (2008)]. The RFEM methodology has been de-
scribed in detail in other publications [e.g., Fenton and Griffiths
(2008)] so only a brief description will be repeated here for the
random variable C_u . An identical procedure is applied to C' and
 $\tan \phi'$.

The lognormally distributed undrained shear strength C_u has
three parameters; the mean μ_{C_u} , the standard deviation σ_{C_u} , and
the spatial correlation length. The variability of C_u can conve-
niently be expressed by the dimensionless coefficient of variation
defined as

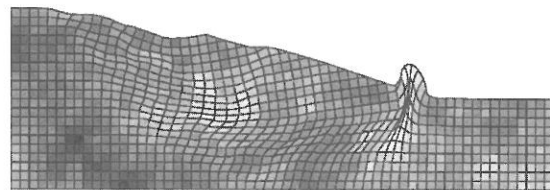
$$v_{C_u} = \frac{\sigma_{C_u}}{\mu_{C_u}} \quad (1)$$

The parameters of the normal distribution (of the logarithm of C_u)
can be obtained from the standard deviation and mean of C_u as
follows:

$$\sigma_{\ln C_u} = \sqrt{\ln 1 + v_{C_u}^2} \quad (2)$$



a) $\Theta_{C_u} = 0.2$



b) $\Theta_{C_u} = 2$

Fig. 2. Influence of the spatial correlation length in RFEM analysis

$$\mu_{\ln C_u} = \ln \mu_{C_u} - \frac{1}{2} \sigma_{\ln C_u}^2 \quad (3)$$

Inverting Eqs. (2) and (3) gives the mean and standard deviation
of C_u

$$\mu_{C_u} = \exp \left(\mu_{\ln C_u} + \frac{1}{2} \sigma_{\ln C_u}^2 \right) \quad (4)$$

$$\sigma_{C_u} = \mu_{C_u} \sqrt{\exp(\sigma_{\ln C_u}^2) - 1} \quad (5)$$

A third parameter, the spatial correlation length $\theta_{\ln C_u}$, will also be
considered in this study. Since the actual undrained shear strength
field is lognormally distributed, its logarithm yields an “underly-
ing” normally distributed (or Gaussian) field. The spatial correla-
tion length is measured with respect to this underlying field, that
is, with respect to $\ln C_u$. In particular, the spatial correlation
length ($\theta_{\ln C_u}$) describes the distance over which the spatially ran-
dom values will tend to be significantly correlated in the under-
lying Gaussian field. Thus, a large value of $\theta_{\ln C_u}$ will imply a
smoothly varying field while a small value will imply a ragged
field.

In this work, an exponentially decaying (Markovian) correla-
tion function is used of the form

$$\rho(\tau) = e^{(-2\tau)/(\theta_{\ln C_u})} \quad (6)$$

where $\rho(\tau)$ =correlation coefficient between properties assigned
to two points in the random field separated by an absolute dis-
tance τ .

In the current study, the spatial correlation length has been
nondimensionalized by dividing it by the height of the embank-
ment H and will be expressed in the form

$$\Theta_{C_u} = \theta_{\ln C_u} / H \quad (7)$$

Figs. 2(a and b) show typical failure mechanisms corresponding
to different spatial correlation lengths. Fig. 2(a) shows a relatively
low spatial correlation length of $\Theta_{C_u}=0.2$ and Fig. 2(b) shows a
relatively high spatial correlation length of $\Theta_{C_u}=2$. The figures
depict the variation in $\ln C_u$ and have been scaled in such a way
that the dark and light regions depict “strong” and “weak” soils,
respectively. Black represents the strongest element and white is
the weakest in the particular realization. It should be emphasized
that both these shear strength distributions come from the same

lognormal distribution (same mean and standard deviation) and it is only the spatial correlation length that is different. A great benefit of RFEM is that the shape and location of the failure surface is not determined a priori and the algorithm is able to “seek out” the most critical path through the heterogeneous soil mass [e.g., Griffiths et al. (2006)].

The input parameters relating to the mean, standard deviation, and spatial correlation length are assumed to be defined at the “point” level. While statistics at this resolution are obviously impossible to measure in practice, they represent a fundamental baseline of the inherent soil variability which can be corrected through local averaging to take account of the sample size. In the context of the RFEM approach, each finite element is assigned a constant property. The “sample” is represented by the size of each finite element used to discretize the slope. If the point distribution is normal, local averaging results in a reduced variance but the mean is unaffected. In a lognormal distribution, however, both the mean and the standard deviation are reduced by local averaging. Following local averaging, the adjusted statistics $\mu_{C_{uA}}$, $\sigma_{C_{uA}}$ represent the mean and standard deviation of the lognormal field that is actually mapped onto the finite-element mesh. Further details can be found in Griffiths and Fenton (2004).

In the limit as $\Theta_{C_u} \rightarrow 0$, local averaging removes all variance ($\sigma_{C_{uA}} \rightarrow 0$) and the mean tends to the median, thus

$$\begin{aligned}\mu_{C_{uA}} &\rightarrow \text{median}_{C_u} = \exp(\mu_{\ln C_u}) \\ &= \exp\left(\ln \mu_{C_u} - \frac{1}{2}\sigma_{\ln C_u}^2\right) = \frac{\mu_{C_u}}{\sqrt{1 + v_{C_u}^2}}\end{aligned}\quad (8)$$

Traditional Probabilistic Methods

Undrained Slope

In this paper, the term “traditional probabilistic methods” refer to the probabilistic methods (whether using Monte Carlo simulation or FORM) which do not explicitly take account of the spatial correlation length, hence, slopes are assumed to be uniform (spatially constant properties) with C_u selected randomly from a lognormal distribution. The traditional probabilistic methods imply a spatial correlation length $\Theta_{C_u} = \infty$ so no local averaging is applicable.

Since there is only one random variable in an undrained analysis, the probability of failure (p_f) is simply equal to the probability that the shear strength parameter C_u will be less than $C_{u,FS=1}$, where $C_{u,FS=1}$ is the value that results in a FS equal to unity. Quantitatively, this equals the area beneath the probability density function corresponding to $C_u \leq C_{u,FS=1}$. For example, for $\alpha = 26.6^\circ$, $C_{u,FS=1} = 0.17$ and $C_{u,FS=1} = 0.25$ (from Taylor’s charts or limit equilibrium) so if we let $\mu_{C_u} = 0.25$ and $\sigma_{C_u} = 0.125$ ($v_{C_u} = 0.5$), Eqs. (2) and (3) give that the mean and standard deviation of the underlying normal distribution are $\mu_{\ln C_u} = -1.489$ and $\sigma_{\ln C_u} = 0.472$, respectively. The probability of failure is therefore given by

$$p_f = p[C_u < 0.17] = \Phi\left(\frac{\ln 0.17 - \mu_{\ln C_u}}{\sigma_{\ln C_u}}\right) = 0.281 \quad (9)$$

where $\Phi \cdot$ = cumulative standard normal distribution function.

In order to investigate the influence of FS on p_f and for $\mu_{C_u} = C_{u,FS=1.25} = 0.21$, $\mu_{C_u} = C_{u,FS=1.47} = 0.25$, and $\mu_{C_u} = C_{u,FS=1.70} = 0.29$, the probability of failure corresponding to different v_{C_u} can be

Table 1. p_f Corresponding to Different v_{C_u} for an Undrained Slope

v_{C_u}	$\mu_{C_u} = C_{u,FS=1.25}$	$\mu_{C_u} = C_{u,FS=1.47}$	$\mu_{C_u} = C_{u,FS=1.70}$
0.1	0.014	0.0	0.0
0.2	0.152	0.032	0.004
0.3	0.270	0.122	0.048
0.4	0.350	0.209	0.118
0.5	0.407	0.281	0.187
0.6	0.450	0.338	0.248
0.7	0.485	0.384	0.300
0.8	0.514	0.422	0.343
0.9	0.538	0.454	0.381
1.0	0.559	0.481	0.412
1.1	0.577	0.505	0.440
1.2	0.593	0.525	0.464
1.3	0.607	0.544	0.485
1.4	0.620	0.560	0.504
1.5	0.632	0.574	0.521

easily obtained and are listed in Table 1. For the purposes of our parametric studies, it was necessary to push the v_{C_u} up as high as 1.5 in some cases in order to find the critical value at which the traditional method ceases to be conservative.

While considering the influence of the slope inclination, it may be noted that in an undrained slope, the slope inclination makes no difference to p_f if FS (based on the mean) is the same in all cases. Thus, the p_f values shown in Table 1 apply to any slope inclination.

FORM and the Hasofer-Lind Reliability Index

The first-order reliability method (FORM) is a process which can be used to estimate the probability of failure of systems involving multiple random variables with given probability density functions, in relation to a “limit state” function that separates the failure domain from the safe domain. Xu and Low (2006) used FORM combined with the finite-element method to estimate the probability of failure of slopes. The conventional FORM based on the Hasofer-Lind reliability index (Hasofer and Lind 1974), β_{HL} , assumes that the mean values of random variables lie on the safe side of the limit state function. The method then obtains the reliability index, which is related to the minimum distance, in directional standard deviation units, between the mean values and the limit state surface. The conceptual and implementation barriers surrounding the use of β_{HL} for correlated normals and the FORM for correlated non-normals can largely be overcome, as shown by Low and Tang (1997a,b, 2004). Calculation of the reliability index involves an iterative optimization process, in which the minimum value of a matrix calculation is found, subject to the constraint that the values are on the limit state surface. Commonly used software packages (e.g., Excel and Matlab) are easily adopted to perform the optimization (see e.g., www.mines.edu/~vgriffit/FORM). Once the reliability index (the distance between the means and the closest failure point) has been determined, the method assumes a “first-order” limit state function tangent to the β contour and the probability of failure p_f follows from:

$$p_f = 1 - \Phi(\beta) \quad (10)$$

It should be noted that the reliability index is given a negative value if $p_f > 50\%$ [e.g., Low (2005)].

If dealing with two random variables, the first-order assumption results in a straight line limit state function, in which case p_f is the volume under the bivariate probability density function on the failure side of the line. A similar concept applies to cases involving multiple random variables.

Each reliability analysis requires a limit state function, which defines safe or unsafe performance. Limit states could relate to strength failure, serviceability failure, or anything else that describes unsatisfactory performance. The limit state function, g , is customarily defined

$$g(X_1, X_2, \dots, X_N) \geq 0 \rightarrow \text{Safe}$$

$$g(X_1, X_2, \dots, X_N) < 0 \rightarrow \text{Failure} \quad (11)$$

where X_1, X_2, \dots, X_N =input random variables. An advantage of the Hasofer-Lind index β_{HL} for correlated normal variates and the FORM index β for correlated non-normal variates is that the result it gives is not affected by the form of the limit state function. For example, the limit state function could be defined as the resistance minus the load, the FS minus one, the logarithm of the FS, or some other algebraic combination without influencing the computed value of β_{HL} or β .

The limit state function can sometimes be determined directly from theory or for more complex systems, the response surface method [e.g., Melchers (1999)] needs to be used. The basic idea of the response surface method is to approximate the limit state boundary by an explicit function of the random variables and to improve the approximation via iterations

In detail, the determination of β in FORM is an iterative process [as explained by Haldar and Mahadevan (2000), for example]. An alternative interpretation involving an equivalent hyperellipsoid was given in Low and Tang (2004) and Low (2005) as follows:

$$\beta = \min_{g=0} \sqrt{\left\{ \frac{X_i - \mu_i^N}{\sigma_i^N} \right\}^T R^{-1} \left\{ \frac{X_i - \mu_i^N}{\sigma_i^N} \right\}} \quad i = 1, 2, \dots, n \quad (12)$$

where X_i = i th random variable, μ_i^N =equivalent normal mean of the i th random variable, σ_i^N =equivalent normal standard deviation of the i th random variable, $\{(X_i - \mu_i^N)/\sigma_i^N\}$ =vector of n random variables reduced to standard normal space, and R =correlation matrix.

Drained Slope

For slopes of $c' - \tan \phi'$ soils, no analytical equation exists which can serve as a limit state function. The response surface method [e.g., Xu and Low (2006)] has been introduced in this study. This can be accomplished, for example, by fitting a curve to the results from several finite-element analyses using the strength reduction method [e.g., Griffiths and Lane (1999)]. This method involves applying gravity loads to the finite-element mesh and systematically weakening the soil until a sufficient number of elements have yielded to allow the formation of a failure mechanism.

For example, with two ($n=2$) random variables, a quadratic surface without cross terms with five ($2n+1=5$) constants of the form

$$\text{FS}(\ln C', \ln(\tan \phi')) = a_1 + a_2 \ln C' + a_3 \ln(\tan \phi') + a_4 (\ln C')^2 + a_5 (\ln(\tan \phi'))^2 \quad (13)$$

could be used to approximate the FS function.

Table 2. Strength Parameters of the Five Slopes

Slope	FS=1.25		FS=1.47		FS=1.70	
	$\mu_{c'}$	$\mu_{\tan \phi'}$	$\mu_{c'}$	$\mu_{\tan \phi'}$	$\mu_{c'}$	$\mu_{\tan \phi'}$
3:1			15.00	0.21		
2:1	15.73	0.23	18.50	0.27	21.40	0.31
1:1			26.00	0.36		

The limit state function could then be defined as the FS function minus one, thus

$$g(\ln C', \ln(\tan \phi')) = \text{FS}(\ln C', \ln(\tan \phi')) - 1 \quad (14)$$

In order to find the five constants in Eq. (13), five finite-element analyses were run. For each random variable, its equivalent normal mean value μ_i^N and two other values $\mu_i^N \pm m\sigma_i^N$ were sampled while fixing the other random variable at its equivalent normal mean value. Some investigators [e.g., Xu and Low (2006) and Griffiths et al. (2007)] have related the two other sampling points to some factor of the standard deviation given by m . A popular choice is $m=1$ which will be used later in this section. For cases involving high v , the use of $m=1$ leads to some sampling points being far from the central sampling point and thus, the performance function may not always be defined with accuracy in the zone of interest (i.e., near the tentative design point). For slope reliability analysis, however, the limit state functions for slopes have been shown to be quite linear in the space of cohesion and friction angle [e.g., Mostyn and Li (1993) and Low et al. (1998)] so p_f is rather insensitive to the choice of m .

Since the design point is not known in advance, the limit state function is initially derived at the equivalent normal mean which gives a first approximation of the design point. This design point can be far from the optimal one and may lead to incorrect results. The current work uses the following iteration procedure [e.g., Tandjiria and Low (2000)], which leads to the limit state function being approximated at the design point.

1. Derive the limit state function at the equivalent normal mean values.
2. Use FORM to obtain the design point and hence p_f .
3. Update the limit state function using the design point just found.
4. Use FORM to update the design point and hence p_f .
5. Repeat 3–4 until convergence when two successive values of p_f is smaller than a prescribed tolerance.

The FS at the design point should equal to one at convergence.

In order to investigate the influence of slope inclination and the FS (based on the mean) on the critical value of coefficient of variation, five slopes have been analyzed using FORM. The mean values that would result in the target FS values for different slope inclinations are shown in Table 2. The investigation will consider a 2:1 slope with three different FS values and a FS=1.47 slope with three different slope inclinations.

In the present work, C' and $\tan \phi'$ are assumed to be lognormally distributed. The mean value of C' can be retrieved from the values in Table 2 as $\mu_{C'} = \mu_{c'}/(\gamma H)$.

Since β is defined in the normal space, transformations of Eqs. (2) and (3) need to be applied and the optimization will be performed in normal space. The five sample points in the normal space will be $(\mu_{\ln C'}, \mu_{\ln(\tan \phi')})$, $(\mu_{\ln C'} + \sigma_{\ln C'}, \mu_{\ln(\tan \phi')})$, $(\mu_{\ln C'} - \sigma_{\ln C'}, \mu_{\ln(\tan \phi')})$, $(\mu_{\ln C'}, \mu_{\ln(\tan \phi')} + \sigma_{\ln(\tan \phi')})$, and $(\mu_{\ln C'}, \mu_{\ln(\tan \phi')} - \sigma_{\ln(\tan \phi')})$.

Since these sample points depend on the input coefficient of variation, five deterministic analyses need to be performed for

Table 3. Coefficients of the Limit State Function for $v=0.5$

Slope	a_1	a_2	a_3	a_4	a_5
2:1, FS=1.25	5.3045	1.6132	1.1186	0.2017	0.1793
2:1, FS=1.47	5.1821	1.5026	1.1212	0.1793	0.1793
2:1, FS=1.70	5.1765	1.5019	1.1204	0.1793	0.1793
3:1, FS=1.47	5.9713	1.5081	1.5442	0.1793	0.2465
1:1, FS=1.47	4.7636	1.8096	0.7733	0.2465	0.1344

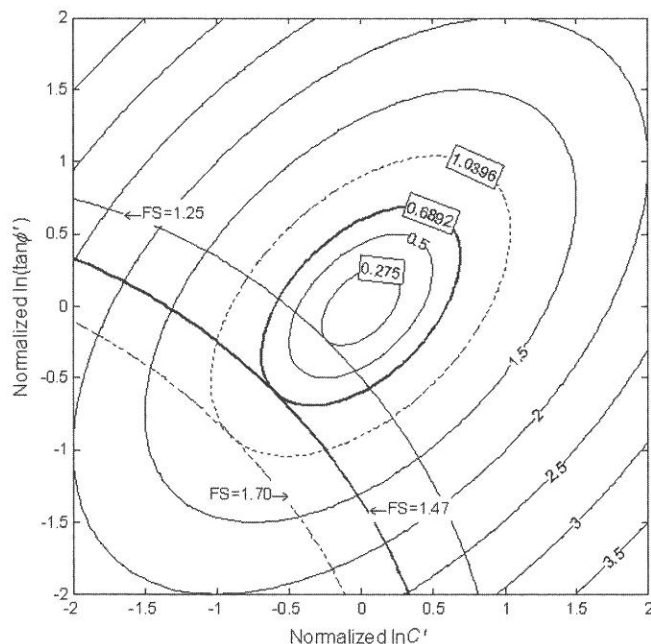
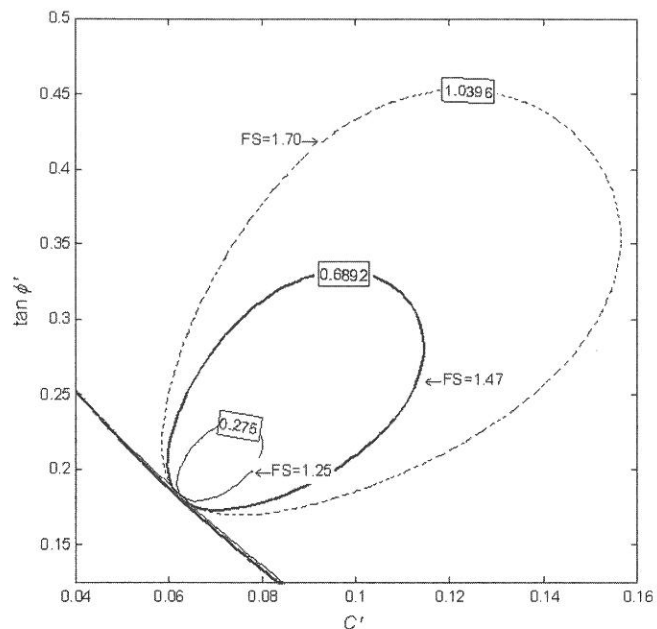
each v . In the present study, for the sake of simplicity, the coefficients of variation relating to cohesion and friction are assumed to be equal, thus

$$v = v_{C'} = v_{\tan \phi'} \quad (15)$$

It may be noted that since the five deterministic analyses must be performed in the real space, actual properties were retrieved by raising e (the base of the natural logarithm) to the five sample points mentioned above. The coefficients of the limit state function for the case when $v=0.5$ used in Eqs. (13) and (14) are shown in Table 3.

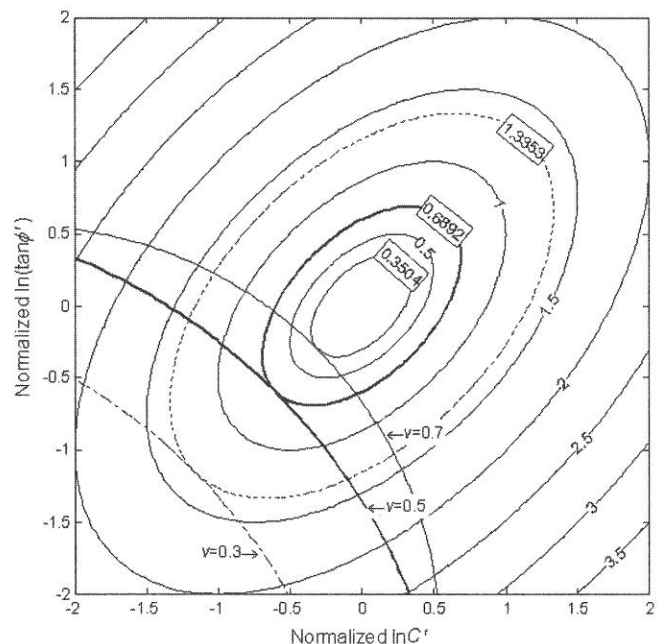
Some investigators [e.g., Rackwitz (2000)] believe that the cross correlation ρ between $\ln C'$ and $\ln(\tan \phi')$ is negative, however, this is still a controversial area in need of a more realistic data. Since a positive cross correlation coefficient (ρ) between $\ln C'$ and $\ln(\tan \phi')$ gives higher values of p_f and is therefore conservative, ρ is initially assigned a value of 0.5, although other values in the range $-0.5 < \rho < 0.5$ are considered later in this paper.

For the case of $v=0.5$, the limit state functions for the 2:1 slope with three different FS values (based on the mean) are shown in the standard normal space along with contours of β in Fig. 3. Also shown in Fig. 3 are the three contours of β that just touch the three limit state functions corresponding to FS=1.25, FS=1.47, and FS=1.70, indicating reliability indices of 0.2750, 0.6892, and 1.0396, respectively. The corresponding p_f are thus determined using Eq. (10) to be 0.392, 0.245, and 0.149. It should

**Fig. 3.** Limit state functions for a 2:1 slope and β contours in standard normal space ($v=0.5$, $\rho=0.5$)**Fig. 4.** Limit state functions for a 2:1 slope and tangent β contours in real space ($v=0.5$, $\rho=0.5$)

be noted that in this standard normal plotting space, the contours of β are functions only of ρ while the limit state function lines are functions of FS and v . The corresponding plot in real space is shown in Fig. 4. In this plotting space, the contours of β are now functions of FS, v , and ρ while the limit states remain functions of FS and v . The proximity of the limit state functions to each other in the real space is striking. Two of the lines are almost identical.

Fig. 5 shows the influence of v on the limit state function in the standard normal space for the case of FS=1.47. It can be seen

**Fig. 5.** Influence of v on the limit state function for a 2:1 slope with FS=1.47 (based on the means) in standard normal space ($\rho=0.5$)

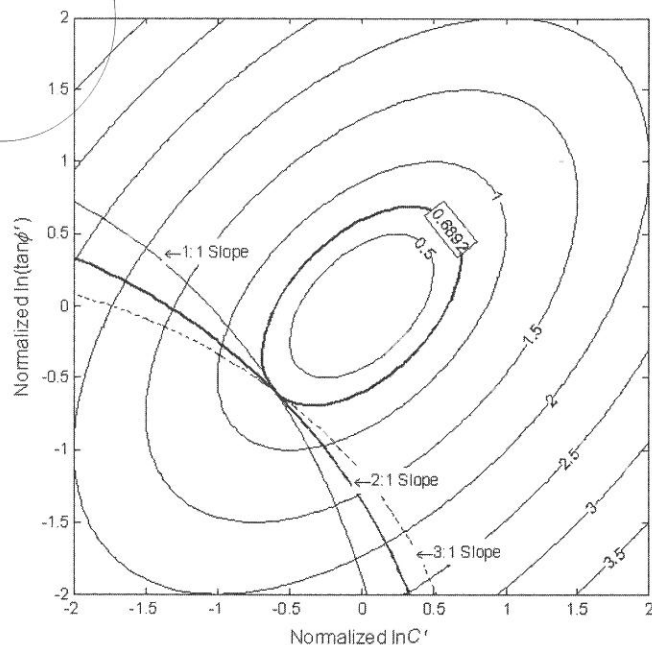


Fig. 6. Influence of slope inclination on the limit state functions for a slope with FS=1.47 (based on the means) in standard normal space ($v=0.5$, $\rho=0.5$)

that larger values of v result in the limit state function being closer to the mean value, indicating lower β and higher p_f values.

The limit state functions in standard normal space for three different slope inclinations are shown in Fig. 6 for the case when FS=1.47. The $\beta=0.6892$ contour is exactly tangent to the 2:1 limit state line but almost tangent to the other two lines, emphasizing again that the slope inclination makes little difference to p_f for slopes with the same FS (based on the mean). Table 4 summarizes the computed p_f for all cases considered.

The influence of ρ on slope probability of failure has also been investigated in this paper. Results shown in Table 5 indicate that when the mean values are on the safe side of the limit state function $p_f < 0.5$ positive ρ is conservative because it gives higher probabilities of failure than negative ρ . If the equivalent normal

Table 4. p_f Corresponding to Different v , FS, and Slope Inclinations

v	FS=1.25 (2:1 slope)	FS=1.47 (2:1 slope)	FS=1.70 (2:1 slope)	FS=1.47 (3:1 slope)	FS=1.47 (1:1 slope)
0.1	0.007	0.000	0.000	0.000	0.000
0.2	0.124	0.015	0.001	0.018	0.017
0.3	0.231	0.091	0.029	0.085	0.091
0.4	0.331	0.167	0.089	0.166	0.169
0.5	0.392	0.245	0.149	0.247	0.248
0.6	0.438	0.319	0.216	0.318	0.321
0.7	0.479	0.363	0.274	0.363	0.365
0.8	0.513	0.409	0.322	0.410	0.408
0.9	0.546	0.441	0.360	0.441	0.442
1.0	0.571	0.475	0.399	0.475	0.475
1.1	0.585	0.509	0.430	0.500	0.509
1.2	0.608	0.527	0.462	0.527	0.527
1.3	0.622	0.549	0.479	0.548	0.548
1.4	0.639	0.569	0.508	0.568	0.568
1.5	0.650	0.588	0.523	0.586	0.587

Table 5. p_f Corresponding to Different ρ and v with FS=1.47 for a 2:1 Slope

v	$\rho=0.5$	$\rho=0.0$	$\rho=-0.5$
0.1	0.000	0.000	0.000
0.2	0.015	0.004	0.000
0.3	0.091	0.051	0.010
0.4	0.167	0.118	0.047
0.5	0.245	0.199	0.116
0.6	0.319	0.282	0.208
0.7	0.363	0.334	0.272
0.8	0.409	0.389	0.345
0.9	0.441	0.428	0.399
1.0	0.475	0.469	0.457
1.1	0.509	0.512	0.516
1.2	0.527	0.533	0.547
1.3	0.549	0.560	0.584
1.4	0.569	0.584	0.618
1.5	0.588	0.607	0.649

mean values lie in the unsafe side of the limit state function $p_f > 0.5$, however, the opposite is true, with positive ρ giving lower probabilities of failure. The explanation lies in the fact that irrespective of the location of the equivalent normal mean values relative to the limit state function, positive ρ always results in the β contours touching the limit state function at lower absolute values of β than when ρ is negative. Since β is interpreted as being positive when $p_f < 0.5$ and negative when $p_f > 0.5$, Eq. (10) will lead to a lower p_f when ρ is positive since the resulting β will be less negative than when ρ is negative.

Figs. 7 and 8 show the influence of ρ when $v=0.5$ and $v=1.5$. The mean values lie in the safe region when $v=0.5$ and the unsafe region when $v=1.5$.

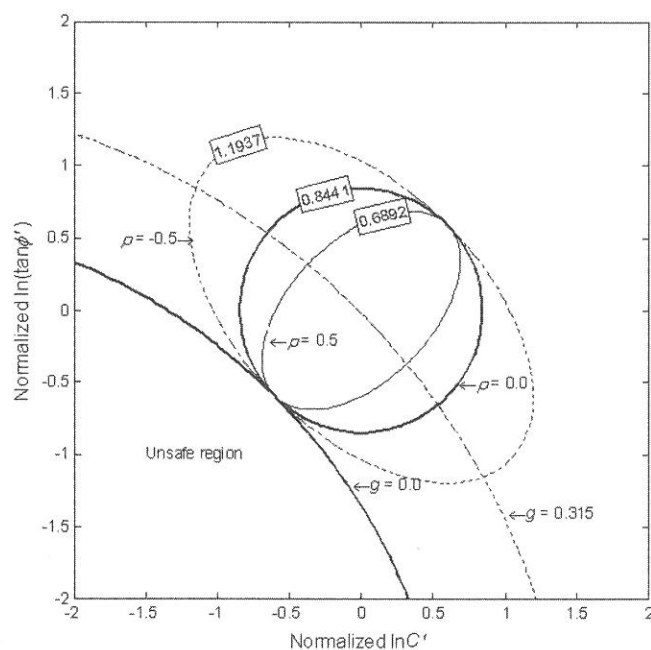


Fig. 7. Influence of ρ on p_f for a 2:1 slope with FS=1.47 (based on the means) in standard normal space when $p_f < 0.5$ and $v=0.5$ (g is performance function)

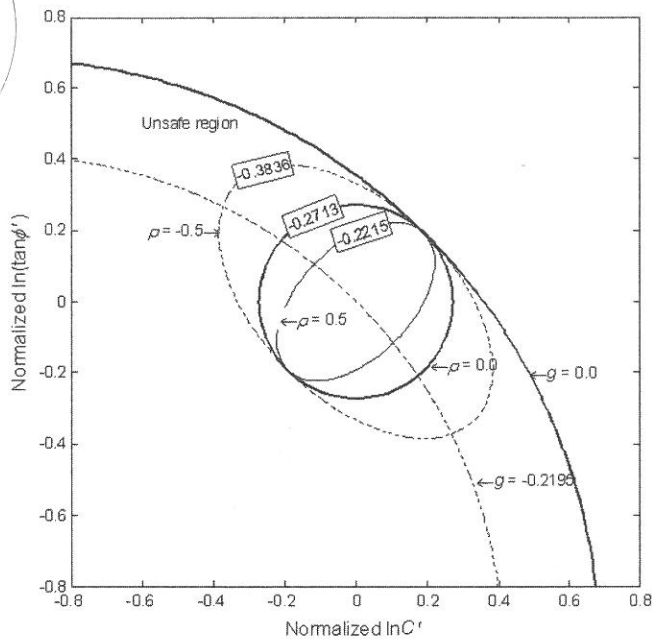


Fig. 8. Influence of ρ on p_f for a 2:1 slope with $FS=1.47$ (based on the means) in standard normal space when $p_f > 0.5$ and $v=1.5$ (g is performance function)

Random Finite-Element Method

In this section, the results of full nonlinear RFEM analyses with Monte Carlo simulations are compared with results from FORM.

The RFEM involves the generation and mapping of a random field of properties onto a finite-element mesh. The current online RFEM codes have implemented only normal, lognormal, and bounded distributions (Fenton and Griffiths 2008). There is no restriction however on the type of distribution that could be modeled by RFEM, provided that a normal transformation is available [e.g., Fig. 5 in Low and Tang (2007)]. Since the random field in RFEM is generated in the underlying normal space, it is easy to map this normal distribution to some other distribution types. Full account is taken of the local averaging and variance reduction (Fenton and Vanmarcke 1990) over each element and an exponentially decaying (Markov) spatial correlation function is incorporated. The random field is initially generated and properties are assigned to the elements. After application of gravity loads, if the algorithm is unable to converge within a user-defined iteration

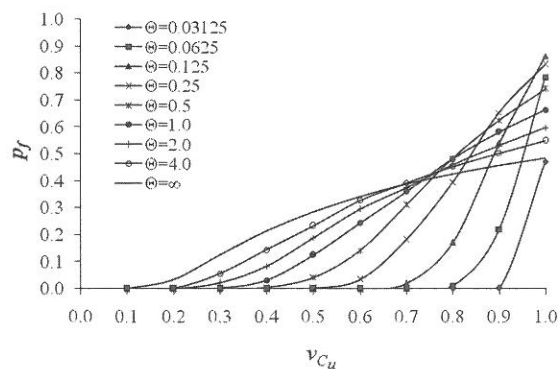


Fig. 9. RFEM results giving p_f of a 3:1 undrained slope with $FS=1.47$ (based on the mean)

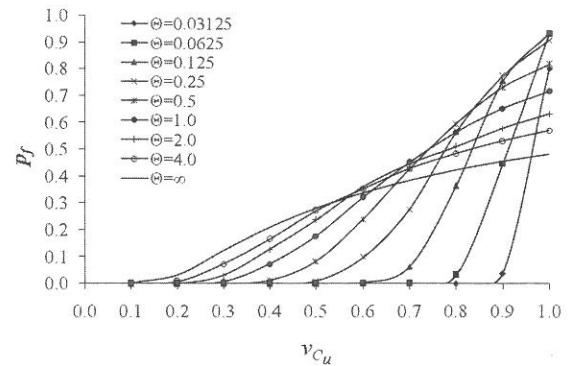


Fig. 10. RFEM results giving p_f of a 2:1 undrained slope with $FS=1.47$ (based on the mean)

ceiling [see, e.g., Griffiths and Lane (1999)], the implication is that no stress distribution can be found that is simultaneously able to satisfy both the Mohr-Coulomb failure criterion and global equilibrium. If the algorithm is unable to satisfy these criteria, failure is said to have occurred. The analysis is repeated numerous times using Monte Carlo simulations. Each realization of the Monte Carlo process involves the same mean, standard deviation, and spatial correlation length of soil properties, however, the spatial distribution of properties varies from one realization to the next. Following a “sufficient” number of realizations, the p_f can be easily estimated by dividing the number of failures by the total number of simulations. The analysis has the option of including cross correlation between properties and anisotropic spatial correlation lengths (e.g., the spatial correlation length in a naturally occurring stratum of soil is often higher in the horizontal direction). Further details of RFEM can be found in Griffiths and Fenton (2004) and Fenton and Griffiths (2008).

A typical mesh is shown in Fig. 2, which has 910 finite elements, and thus contains 910 random variables for an undrained $\phi_u=0$ slope and 1,820 for a drained c', ϕ' slope. The 2,000 simulations were used in most cases while 5,000 simulations were used for high spatial correlation lengths ($\Theta \geq 1.0$) and high input coefficients of variation ($v \geq 1.0$). The aim of this paper is to find v_{crit} and the minimum corresponding value of p_f observed in the parametric studies was about 10%. If the maximum error of p_f is 0.01 at a confidence level 90%, the required number of realization is 2,435 [see, e.g., Fenton and Griffiths (2008)]. It can therefore be said that 2,000 simulations is nearly adequate to achieve this target error bound. The CPU time depends on p_f and runs to about

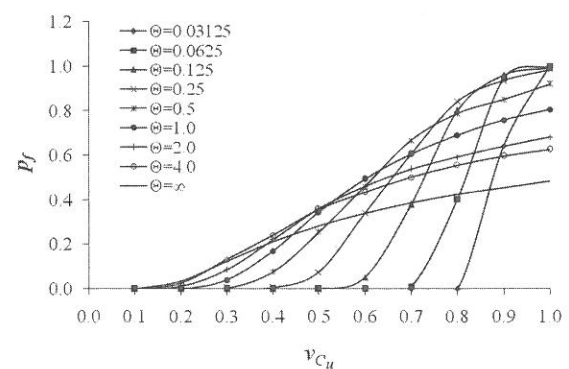


Fig. 11. RFEM results giving p_f of a 1:1 undrained slope with $FS=1.47$ (based on the mean)

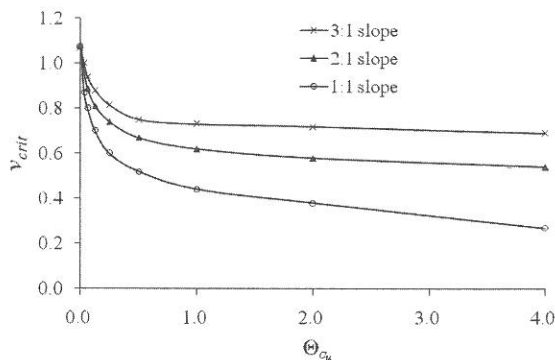


Fig. 12. v_{crit} vs Θ_{C_u} for different inclinations of an undrained slope with $FS=1.47$ (based on the mean)

10 min if $p_f=0$ and 2h if $p_f=1$ (every simulation hits the iteration ceiling) on a T7700@2.4GHz laptop for 2,000 simulations.

Undrained $\phi_u=0$ Slope

The value of μ_{C_u} was fixed at $C_{u,FS=1.47}$ while v_{C_u} was varied in the range $v_{C_u}=0.1, 0.2, \dots, 1.0$ and Θ_{C_u} was varied in the range $\Theta_{C_u}=\{1/32, 1/16, \dots, 4\}$. Figs. 9–11 show the probability of failure estimated by RFEM for the three slopes compared with the $\Theta_{C_u}=\infty$ result obtained by FORM or Monte Carlo simulations.

It can be seen that ignoring spatial variation underestimates the probability of failure when v_{C_u} is relatively high and overestimates the probability of failure when v_{C_u} is relatively low. The intersections of the $\Theta_{C_u}=\infty$ line with other lines gives the v_{crit} at which the $\Theta_{C_u}=\infty$ approach (i.e., no spatial variation) ceases to be conservative. A plot of v_{crit} versus Θ_{C_u} is shown in Fig. 12. It can be seen that ignoring spatial variation will underestimate the probability of failure at lower values of v_{crit} for steeper slopes than for flatter slopes. In the case of steeper slopes, v_{crit} could be as low as 0.27. Typical ranges of v_{C_u} , as reported for example by Lee et al. (1983), Lacasse and Nadim (1996), and Lumb (1974), are 0.05–0.5. It may be noted that from Fig. 12, ignoring spatial variation will always underestimate p_f for a 1:1 slope when $\Theta_{C_u} > 0.5$.

If spatial variation is ignored, the slope inclination made no difference to p_f if FS (based on the mean) is the same in all cases but using RFEM, the p_f of a steeper slope was higher than that of flatter slope. The reason for this is that RFEM allows the failure

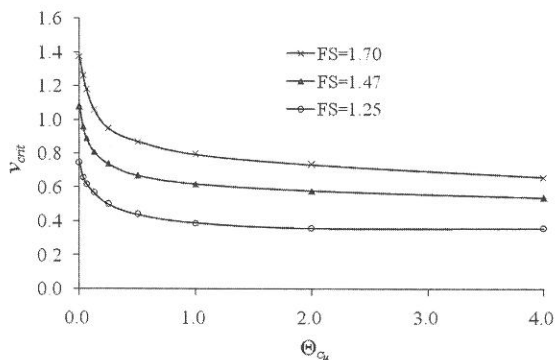


Fig. 13. v_{crit} vs Θ_{C_u} for different FS values (based on the mean) for a 2:1 undrained slope

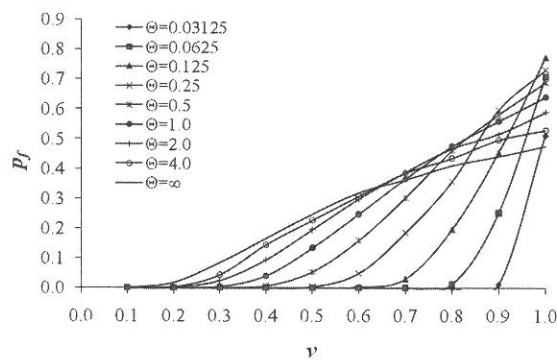


Fig. 14. RFEM results giving p_f of a 3:1 drained slope with $FS=1.47$ (based on the means) $\rho=0.5$

mechanism to seek out the most critical path through the heterogeneous soil mass. For flatter undrained slopes, the failure mechanism is nearly always deep and passes through the foundation soils. For steeper slopes, the failure mechanism has more choices and may go through the toe or pass through the deeper foundation soils, leading to a higher p_f .

In order to investigate the influence of the FS on a single slope, similar computations were carried out for 2:1 slopes with $\mu_{C_u}=C_{u,FS=1.25}$ and $\mu_{C_u}=C_{u,FS=1.70}$. Results in Fig. 13 show that ignoring spatial variation will underestimate the probability of failure at lower values of v_{crit} for low FS slopes than high FS slopes, where FS is based on the mean.

It should be noted that the v_{crit} corresponding to $\Theta_{C_u}=0.0$ in each case was obtained analytically from Eq. (8). The v_{crit} in these cases is the value that causes the median to equal $C_{u,FS=1.0}$.

Drained $C' - \tan \phi'$ Slope

The spatial correlation lengths of C' and $\tan \phi'$ are assumed to be the same. That is

$$\Theta = \Theta_{C'} = \Theta_{\tan \phi'} \quad (16)$$

and all other parameters are varied in the same range as in the previous section. Figs. 14–16 show the probability of failure computed by RFEM for the three slopes with the $\Theta=\infty$ results obtained by FORM or Monte Carlo simulations.

It can be seen from Figs. 14–16 that the slope inclination has little influence on the p_f and that ignoring the spatial variation underestimates the probability of failure when v is relatively high and overestimates the probability of failure when v is relatively

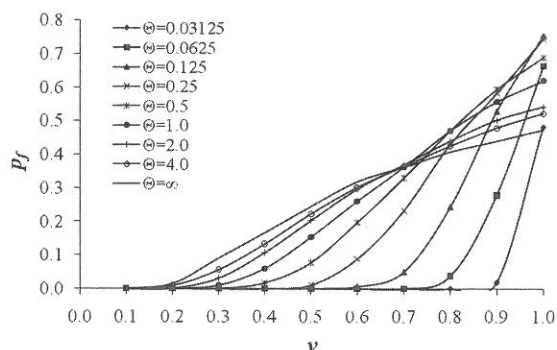


Fig. 15. RFEM results giving p_f of a 2:1 drained slope with $FS=1.47$ (based on the means) $\rho=0.5$

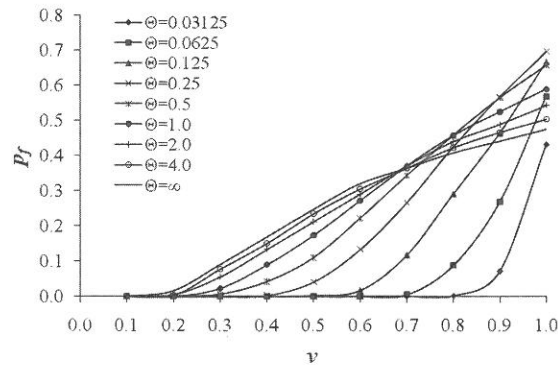


Fig. 16. RFEM results giving p_f of a 1:1 drained slope with FS = 1.47 (based on the means) $\rho = 0.5$

low. The intersections of the $\Theta = \infty$ line with other lines give the v_{crit} above which the $\Theta = \infty$ approach (i.e., ignoring spatial variation) ceases to be conservative. The v_{crit} versus Θ relationship is plotted in Fig. 17, which demonstrates that the v_{crit} is almost independent of the slope inclination. This is different from the undrained slope where v_{crit} was lower for steeper slopes. The RFEM results are less sensitive to slope inclination and more like those given by ignoring spatial variation for drained (c', ϕ') slopes than undrained slopes because the failure mechanism for nearly all slope inclinations tends to pass through the toe.

In order to investigate the influence of the FS (based on the means), similar computations were carried out for 2:1 slopes with FS = 1.25 and FS = 1.70. Results in Fig. 18 show that v_{crit} is lower for low FS slopes (based on the mean). This is a similar trend to that observed in undrained slopes.

Finally, the influence of the cross correlation between $\ln C'$ and $\ln(\tan \phi')$ was investigated, for 2:1 slopes by performing additional RFEM runs with $\rho = 0$ and $\rho = -0.5$. Results in Fig. 19 show that v_{crit} is lower when $\ln C'$ and $\ln(\tan \phi')$ are positively correlated than when they are negatively correlated. It should be noted that RFEM always gave the highest p_f when $\rho = 0.5$ and the lowest p_f when $\rho = -0.5$ irrespective of whether $p_f > 0.5$ or $p_f < 0.5$. Ignoring spatial variation, however, gave the opposite trend for $p_f > 0.5$ and $p_f < 0.5$ as described previously.

The range of $v_{\phi'}$ reported, for example by Lee et al. (1983), Lacasse and Nadim (1996), and Lumb (1974), is 0.02–0.56 (the corresponding range of $v_{\tan \phi'}$ would be 0.03–0.74 when

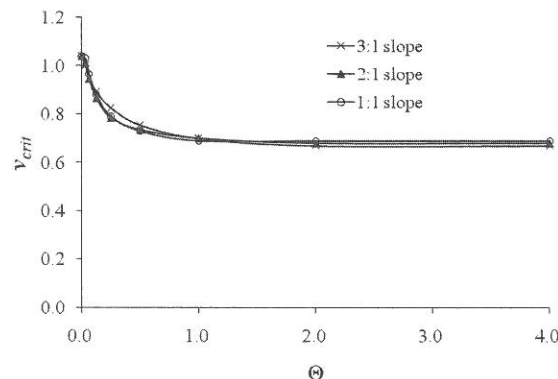


Fig. 17. v_{crit} vs Θ for different slope inclinations for a drained slope with FS = 1.47 (based on the means) $\rho = 0.5$

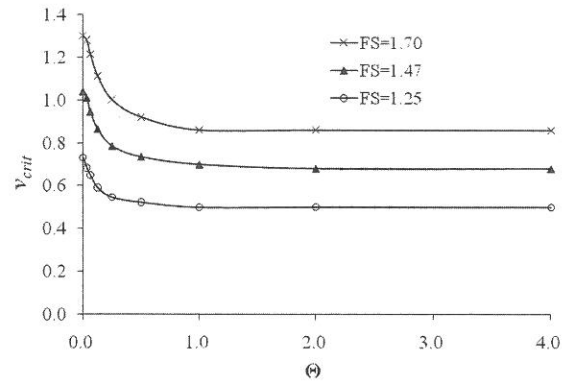


Fig. 18. v_{crit} vs Θ for different FS values (based on the means) for a 2:1 drained slope $\rho = 0.5$

$\phi' = 30^\circ$). It was observed that v_{crit} was higher when ρ was negative than when it was positive, as shown in Fig. 19. Some investigators [e.g., Rackwitz (2000)] have suggested that $\rho \approx -0.5$. The minimum v_{crit} obtained in this paper (based on $\tan \phi'$) is 0.56 for the 2:1 drained slope with FS = 1.25 and a positive $\rho = 0.5$. Lower v_{crit} values will be observed in steeper slopes and/or slopes with lower FS.

It should be noted that the v_{crit} corresponding to $\Theta = 0.0$ can be obtained analytically. As shown in Eq. (8), in the limit as $\Theta \rightarrow 0$, local averaging removes all variance and the mean tends to the Median, thus

$$\mu_{C'A} = \frac{\mu_{C'}}{\sqrt{1 + v_{crit}^2}} \quad (17)$$

$$\mu_{\tan \phi'A} = \frac{\mu_{\tan \phi'}}{\sqrt{1 + v_{crit}^2}} \quad (18)$$

where the subscript A denotes a local average. In this case, the slope will be uniform with the strength parameters set equal to their median as given by Eqs. (17) and (18) everywhere. The value of v_{crit} that would give FS = 1.0 can be obtained by substituting Eqs. (17) and (18) into Eq. (13)

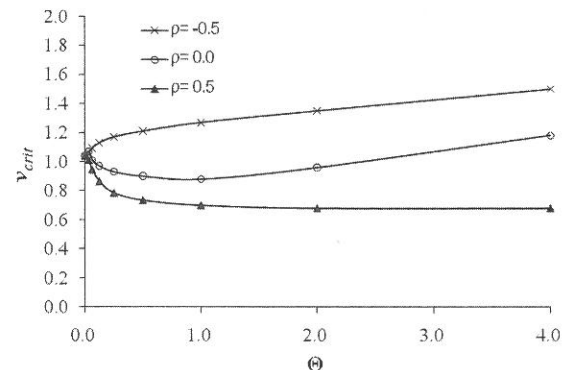


Fig. 19. v_{crit} vs Θ for different ρ values for a 2:1 drained slope with FS = 1.47 (based on the means)

$$\begin{aligned}
& \text{FS}(\ln \mu_{c'A}, \ln(\mu_{\tan \phi'A})) \\
&= a_1 + a_2 \ln \left(\frac{\mu_{C'}}{\sqrt{1 + v_{\text{crit}}^2}} \right) + a_3 \ln \left(\frac{\mu_{\tan \phi'}}{\sqrt{1 + v_{\text{crit}}^2}} \right) \\
&+ a_4 \left(\ln \left(\frac{\mu_{C'}}{\sqrt{1 + v_{\text{crit}}^2}} \right) \right)^2 + a_5 \left(\ln \left(\frac{\mu_{\tan \phi'}}{\sqrt{1 + v_{\text{crit}}^2}} \right) \right)^2 = 1.0
\end{aligned}
\tag{19}$$

The five coefficients a_1, a_2, \dots, a_5 depend on v so an iterative process has been used to solve Eq. (19). The solution gives the value of v_{crit} below which $p_f=0$ and above which $p_f=1$.

Concluding Remarks

The paper has investigated the probability of slope failure using FEM combined with FORM without spatial variation and more advanced (RFEM) probabilistic analysis tools. The term RFEM denotes FEM combined with Monte Carlo simulation with spatial variation are properly taken into account. The RFEM enables the failure mechanism to seek out the weakest path through the heterogeneous soil mass which can lead to higher probabilities of failure than would be predicted by ignoring spatial variation. The numerical studies have shown that ignoring spatial variation will lead to unconservative estimates of the probability of slope failure if the coefficient of variation of the input shear strength parameters exceeds a critical value v_{crit} . The lower the value of v_{crit} , the more likely it is that ignoring spatial variation will underestimate the probability of failure for typical ranges of soil variability. The paper has presented graphs to indicate the magnitude of v_{crit} for different parametric combinations, from which the readers can decide whether ignoring spatial variation (i.e., assuming perfect spatial correlation) is appropriate and conservative for use with their specific soil parameters. The lognormal distribution, as used in this study, is believed to be a reasonable model of soil strength although a thorough comparison of distribution types in the context of RFEM is a topic for future research.

In summary

1. v_{crit} is lower for slopes with low factors of safety (based on the mean) than for slopes with high factors of safety.
2. v_{crit} is lower for steeper slopes than less steep slopes under undrained $\phi_u=0$ conditions. Slope steepness was found to have little influence on v_{crit} in drained c', ϕ' slopes.
3. v_{crit} is lower if the strength parameters c' and $\tan \phi'$ are positively correlated than if they are negatively correlated.

Acknowledgments

The writers acknowledge the support of NSF (Grant No. CMS-0408150) on "Advanced probabilistic analysis of stability problems in geotechnical engineering."

Notation

The following symbols are used in this paper:

C_u = dimensionless undrained cohesion;
 $C_{u, \text{FS}=1}$ = dimensionless undrained cohesion when FS = 1.0;

$C_{u, \text{FS}=1.25}$ = dimensionless undrained cohesion when FS = 1.25;
 $C_{u, \text{FS}=1.47}$ = dimensionless undrained cohesion when FS = 1.47;
 $C_{u, \text{FS}=1.70}$ = dimensionless undrained cohesion when FS = 1.70;
 C' = dimensionless drained cohesion;
 c_u = undrained cohesion;
 c' = drained cohesion;
 D = foundation depth ratio;
 FS = factor of safety;
 H = slope height;
 m = constant used for sampling limit state function;
 n = number of random variables;
 p_f = probability of failure;
 R = correlation matrix;
 v = coefficient of variation;
 $v_{C'}$ = coefficient of variation of dimensionless drained cohesion;
 v_{C_u} = coefficient of variation of dimensionless undrained cohesion;
 v_{crit} = critical coefficient of variation;
 $v_{\tan \phi'}$ = coefficient of variation of tangent drained friction angle;
 X_i = random variable;
 α = slope angle;
 β = FORM reliability index;
 β_{HL} = the Hasofer-Lind reliability index;
 γ = soil unit weight;
 γ_{sat} = saturated soil unit weight;
 Θ = dimensionless spatial correlation length;
 Θ_{C_u} = dimensionless spatial correlation length of undrained cohesion;
 $\Theta_{C'}$ = dimensionless spatial correlation length of drained cohesion;
 $\Theta_{\tan \phi'}$ = dimensionless spatial correlation length of drained tangent friction angle;
 $\theta_{\ln C_u}$ = spatial correlation length of undrained cohesion;
 $\mu_{C_{uA}}$ = mean dimensionless undrained cohesion after local averaging;
 $\mu_{C'A}$ = mean dimensionless drained cohesion after local averaging;
 $\mu_{\ln C_u}$ = equivalent normal mean of undrained cohesion;
 μ_i^N = equivalent normal mean of the i th random variable;
 $\mu_{\tan \phi'A}$ = mean tangent drained friction angle after local averaging;
 ρ = cross correlation coefficient;
 $\rho(\tau)$ = correlation coefficient between properties assigned to two points;
 σ_{C_u} = standard deviation of dimensionless undrained cohesion;
 $\sigma_{C_{uA}}$ = standard deviation of dimensionless undrained cohesion after local averaging;
 $\sigma_{\ln C_u}$ = equivalent normal standard deviation of undrained cohesion;
 σ_i^N = equivalent normal standard deviation of the i th random variable;
 τ = absolute distance between two points in a random field;
 $\Phi \bullet$ = cumulative standard normal distribution function;

ϕ_u = undrained friction angle; and
 ϕ' = drained friction angle.

References

- Alonso, E. E. (1976). "Risk analysis of slopes and its application to slopes in Canadian sensitive clays." *Geotechnique*, 26, 453–472.
- Babu, G. L. S., and Mukesh, M. D. (2004). "Effect of soil variability on reliability of soil slopes." *Geotechnique*, 54(5), 335–337.
- Bhattacharya, G., Jana, D., Ojha, S., and Chakraborty, S. (2003). "Direct search for minimum reliability index of earth slopes." *Comput. Geotech.*, 30(6), 455–462.
- Cho, S. E. (2007). "Effects of spatial variability of soil properties on slope stability." *Eng. Geol.*, 92(3–4), 97–109.
- Chowdhury, R. N., and Tang, W. H. (1987). "Comparison of risk models for slopes." *Proc., 5th Int. Conf. on Applications of Statistics and Probability in Soil and Structural Engineering*, Vol. 2, Univ. of British Columbia, Vancouver, BC, Canada, 863–869.
- Chowdhury, R. N., and Xu, D. W. (1995). "Geotechnical system reliability of slopes." *Reliab. Eng. Syst. Saf.*, 47, 141–151.
- Christian, J. T. (1996). "Reliability methods for stability of existing slopes." *Proc., Uncertainty in the Geologic Environment: From Theory to Practice*, C. D. Shackelford, P. P. Nelson, and M. J. S. Roth, eds., ASCE, Reston, Va., 409–419.
- Christian, J. T., Ladd, C. C., and Baecher, G. B. (1994). "Reliability applied to slope stability analysis." *J. Geotech. Engrg.*, 120(12), 2180–2207.
- D'Andrea, R. A., and Sangrey, D. A. (1982). "Safety factors for probabilistic slope design." *J. Geotech. Engrg. Div.*, 108(9), 1108–1118.
- Duncan, J. M. (2000). "Factors of safety and reliability in geotechnical engineering." *J. Geotech. Geoenviron. Eng.*, 126(4), 307–316.
- El-Ramly, H., Morgenstern, N. R., and Cruden, D. M. (2002). "Probabilistic slope stability analysis for practice." *Can. Geotech. J.*, 39, 665–683.
- Fenton, G. A., and Griffiths, D. V. (2008). *Risk assessment in geotechnical engineering*, Wiley, New York.
- Fenton, G. A., and Vanmarcke, E. H. (1990). "Simulation of random fields via local average subdivision." *J. Eng. Mech.*, 116(8), 1733–1749.
- Griffiths, D. V., and Fenton, G. A. (2004). "Probabilistic slope stability analysis by finite elements." *J. Geotech. Geoenviron. Eng.*, 130(5), 507–518.
- Griffiths, D. V., Fenton, G. A., and Denavit, M. D. (2007). "Traditional and advanced probabilistic slope stability analysis." *Proc., Geo-Denver 2007 Symp.*, K. K. Phoon, G. A. Fenton, E. F. Glynn, C. H. Juang, D. V. Griffiths, T. F. Wolff, and L. Zhang, eds., ASCE, Reston, Va., 1–10.
- Griffiths, D. V., Fenton, G. A., and Ziemann, H. R. (2006). "Seeking out failure: The random finite element method (RFEM) in probabilistic geotechnical analysis." *Proc., Mini-Symp. on Numerical Modeling and Analysis (Probabilistic Modeling and Design)*, ASCE, Reston, Va.
- Griffiths, D. V., and Lane, P. A. (1999). "Slope stability analysis by finite elements." *Geotechnique*, 49(3), 387–403.
- Haldar, A., and Mahadevan, S. (2000). *Reliability assessment using stochastic finite element analysis*, Wiley, New York.
- Hasofer, A. M., and Lind, N. C. (1974). "Exact and invariant second moment code format." *J. Engrg. Mech. Div.*, 100(1), 111–121.
- Hassan, A. M., and Wolff, T. F. (1999). "Search algorithm for minimum reliability index of earth slopes." *J. Geotech. Geoenviron. Eng.*, 125(4), 301–308.
- Lacasse, S. (1994). "Reliability and probabilistic methods." *Proc., 13th Int. Conf. Soil Mechanics and Foundation Engineering*, New Delhi, India, 225–227.
- Lacasse, S., and Nadim, F. (1996). "Uncertainties in characterizing soil properties." *Proc., Uncertainty 1996*, C. D. Shackelford, P. P. Nelson, and M. J. S. Roth, eds., ASCE, Reston, Va., 49–75.
- Lee, I. K., White, W., and Ingles, O. G. (1983). *Geotechnical engineering*, Pitman, London.
- Li, K. S., and Lumb, P. (1987). "Probabilistic design of slopes." *Can. Geotech. J.*, 24, 520–531.
- Low, B. K. (1996). "Practical probabilistic approach using spreadsheet." *Proc., Uncertainty in the Geologic Environment: From Theory to Practice*, Vol. 2, Reston, Va., 1284–1302.
- Low, B. K. (2003). "Practical probabilistic slope stability analysis." *Proc., Soil and Rock America 2003, 12th Panamerican Conf. on Soil Mechanics and Geotechnical Engineering, and 39th U.S. Rock Mechanics Symp.*, MIT, Cambridge, Mass., Vol. 2, Verlag Glückauf GmbH, Essen, Germany, 2777–2784.
- Low, B. K. (2005). "Reliability-based design applied to retaining walls." *Geotechnique*, 55(1), 63–75.
- Low, B. K., Gilbert, R. B., and Wright, S. G. (1998). "Slope reliability analysis using generalized method of slices." *J. Geotech. Geoenviron. Eng.*, 124(4), 350–362.
- Low, B. K., Lacasse, S., and Nadim, F. (2007). "Slope reliability analysis accounting for spatial variation." *Georisk*, Vol. 1, Taylor and Francis, London, 177–189.
- Low, B. K., and Tang, W. H. (1997a). "Reliability analysis of reinforced embankments on soft ground." *Can. Geotech. J.*, 34(5), 672–685.
- Low, B. K., and Tang, W. H. (1997b). "Efficient reliability evaluation using spreadsheet." *J. Geotech. Geoenviron. Eng.*, 123(7), 749–752.
- Low, B. K., and Tang, W. H. (2004). "Reliability analysis using object-oriented constrained optimization." *Struct. Safety*, 26(1), 69–89.
- Low, B. K., and Tang, W. H. (2007). "Efficient spreadsheet algorithm for first-order reliability method." *J. Geotech. Geoenviron. Eng.*, 133(12), 1378–1387.
- Lumb, P. (1974). "Application of statistics in soil mechanics." *Soil mechanics: New horizons*, I. K. Lee, ed., Butterworth's, London.
- Massih, D. S. Y. A., Soubra, A.-H., and Low, B. K. (2008). "Reliability-based analysis and design of strip footings against bearing capacity failure." *J. Geotech. Geoenviron. Eng.*, 134(7), 917–928.
- Matsuo, M., and Kuroda, K. (1974). "Probabilistic approach to the design of embankments." *Soils Found.*, 14(1), 1–17.
- Melchers, R. E. (1999). *Structural reliability analysis and prediction*, Wiley, New York.
- Mostyn, G. R., and Li, K. S. (1993). "Probabilistic slope stability—State of play." *Proc., Conf. Probabilistic Meth. Geotech. Eng.*, K. S. Li and S.-C. R. Lo, eds., Balkema, Rotterdam, The Netherlands, 89–110.
- Mostyn, G. R., and Soo, S. (1992). "The effect of autocorrelation on the probability of failure of slopes." *Proc., 6th Australia, New Zealand Conf. on Geomechanics: Geotechnical Risk*, 542–546.
- Nour, A., Slimani, A., and Laouami, N. (2002). "Foundation settlement statistics via finite element analysis." *Comput. Geotech.*, 29, 641–672.
- Oka, Y., and Wu, T. H. (1990). "System reliability of slope stability." *J. Geotech. Engrg.*, 116, 1185–1189.
- Parkin, T. B., Meisinger, J. J., Chester, S. T., Starr, J. L., and Robinson, J. A. (1988). "Evaluation of statistical methods for lognormally distributed variables." *Soil Sci. Soc. Am. J.*, 52, 323–329.
- Parkin, T. B., and Robinson, J. A. (1992). "Analysis of lognormal data." *Adv. Soil Sci.*, 20, 193–235.
- Rackwitz, R. (2000). "Reviewing probabilistic soils modeling." *Comput. Geotech.*, 26(3–4), 199–223.
- Shinoda, M. (2007). "Quasi-Monte Carlo simulation with low-discrepancy sequence for reinforced soil slopes." *J. Geotech. Geoenviron. Eng.*, 133(4), 393–404.
- Tandjiria, V., Teh, C. I., and Low, B. K. (2000). "Reliability analysis of laterally loaded piles using response surface methods." *Struct. Safety*, 22(4), 335–355.
- Tang, W. H., Yucemen, M. S., and Ang, A. H. S. (1976). "Probability based short-term design of slopes." *Can. Geotech. J.*, 13, 201–215.

- Theory manual of slope/W 2007 version.* (2007). GEO-SLOPE International Ltd., Alberta, Canada, (<http://www.geo-slope.com/downloads/2007.aspx>) (Aug. 9, 2008).
- Vanmarcke, E. H. (1977). "Reliability of earth slopes." *J. Geotech. Engrg. Div.*, 103(11), 1247–1265.
- Whitman, R. V. (2000). "Organizing and evaluating in geotechnical engineering." *J. Geotech. Geoenviron. Eng.*, 126(7), 583–593.
- Wolff, T. F. (1996). "Probabilistic slope stability in theory and practice." *Uncertainty in the geologic environment: From theory to practice*, C. D. Shackelford, P. P. Nelson, and M. J. S. Roth, eds., ASCE, Reston, Va., 419–433.
- Xu, B., and Low, B. K. (2006). "Probabilistic stability analyses of embankments based on finite-element method." *J. Geotech. Geoenviron. Eng.*, 132(11), 1444–1454.